Available online at www.sciencedirect.com
ScienceDirect
Physica B 403 (2008) 539–543
PHYSICA B
www.elsevier.com/locate/physb

First-principles study of structural, elastic, electronic, and optical properties of hexagonal $BiAlO_3$

Chenliang Li[a], Biao Wang[a,b,*], Rui Wang[c], Hai Wang[a], Xiaoyan Lu[a]

[a]School of Astronautics, Harbin Institute of Technology, Harbin, China
[b]State Key Laboratory of Optoelectronic Materials and Technologies, Institute of Optoelectronic and Functional Composite Materials, School of Physics and Engineering, Sun Yat-sen University, Guangzhou, China
[c]Department of Applied Chemistry, Harbin Institute of Technology, Harbin, China

Received 4 July 2007; received in revised form 30 August 2007; accepted 1 September 2007

Abstract

The structural parameters, elastic, electronic, and optical properties of hexagonal $BiAlO_3$ were investigated by the density functional theory. The calculated structural parameters are in good agreement with previous calculation and experimental data. The structural stability of $BiAlO_3$ has been confirmed by calculation of the elastic constants. The energy band structure, density of states, and Mulliken charge populations were obtained. $BiAlO_3$ presents an indirect band gap of 3.28 eV. Furthermore, the optical properties were calculated and analyzed. It is shown that $BiAlO_3$ is a promising dielectric material.

PACS: 71.15.Mb; 73.20.At; 74.25.Gz; 78.20.Ci

Keywords: Density functional theory; Structural properties; Elastic constants; Electronic properties; Optical properties

1. Introduction

$BiMO_3$ (M = Mn, Fe, Al, Ga, Sc, In) has received tremendous attention as multiferroics and in the research of $BiMO_3$–$PbTiO_3$ solid solutions to halve the amount of lead and obtain new morphotropic phase boundary piezoelectrics [1–8]. Recently, Baetting et al. [9] theoretically predicted the large ferroelectric polarization and piezoelectricity in the hypothetical perovskite-structure oxides $BiAlO_3$. They proposed the $BiAlO_3$ system as a replacement for the widely used piezoelectric material, $Pb(Zr,Ti)O_3$ (PZT), that will avoid the environmental toxicity problems of lead-based compounds. Therefore, the studies on the crystal structure and related physical properties of $BiAlO_3$ are of great interest. Belik et al. [10] prepared $BiAlO_3$ under high-pressure high-temperature technique. It is reported that $BiAlO_3$ has the hexagonal structure closely related to that of multiferroic perovskite-like $BiFeO_3$. Moreover, $BiAlO_3$ has a noncentrosymmetric structure. Noncentrosymmetric compounds have important properties, such as piezoelectricity, ferroelectricity, pyroelectricity, as well as second-order nonlinear optical behavior. Furthermore, to understand the origin of ferroelectricity in $BiMO_3$ materials, Wang et al. [11] studied the structures, energy bands, and density of states of cubic $BiAlO_3$ using the full potential linearized augmented plane wave (FP-LAPW) method. However, the properties of hexagonal $BiAlO_3$ were not studied theoretically.

In this work, we focus on the structure, elastic constants, electronic, and optical properties of hexagonal $BiAlO_3$ using the first-principles density functional theory (DFT). We think that it is worthwhile to perform these calculations for completing the exciting experimental and theoretical works for $BiAlO_3$.

2. Computational details

Geometry optimization and properties of hexagonal $BiAlO_3$ were performed using the plane-wave pseudopotential method

*Corresponding author. School of Astronautics, Harbin Institute of Technology, Harbin 150001, China. Tel./fax: +86 20 84115692.
E-mail address: lichenliang1980@yahoo.com.cn (B. Wang).

0921-4526/$ - see front matter © 2007 Elsevier B.V. All rights reserved.
doi:10.1016/j.physb.2007.09.057

based on the DFT with the generalized gradient approximation (GGA) in the scheme of Perdew et al. [12]. Only valence electrons were taken into account, corresponding to Bi $6s^26p^3$, Al $3s^23p^1$, and O $2s^22p^4$ electronic configurations. Ultrasoft Vanderbilt-type pseudopotentials were used [13]. Mulliken charges were calculated according to the formalism described by Segall et al. [14]. A plane-wave cutoff energy of 400 eV was employed throughout the calculation. To check the accuracy of our results, we have increased the energy cutoff from 400 to 600 eV. The total energy of the unit cell changed from −9186.94 to −9187.98 eV, and the first three decimal digits of the lattice parameters do not change at all. Geometry optimization was achieved using convergence thresholds of 1×10^{-5} eV/atom for total energy, 0.03 eV/Å for maximum force, 0.05 GPa for pressure, and 0.001 Å for displacement. The tolerance in the self-consistent field (SCF) calculation is 1.0×10^{-6} eV/atom. For the sampling of the Brillouin zone, the electronic structures and optical properties used a $8\times8\times6$ and $10\times10\times8$ k-point grid generated according to the Monkhorst–Pack scheme [15], respectively. The elastic constants were calculated by the 'stress–strain' method.

The optical properties of $BiAlO_3$ are determined by the frequency-dependent dielectric function $\varepsilon(\omega)=\varepsilon_1(\omega)+i\varepsilon_2(\omega)$ that is mainly connected with the electronic structures. The imaginary part $\varepsilon_2(\omega)$ of the dielectric function $\varepsilon(\omega)$ is calculated from the momentum matrix elements between the occupied and unoccupied electronic states and given by

$$\varepsilon_2=\frac{2e^2\pi}{\Omega\varepsilon_0}\sum_{k,v,c}\left|\langle\psi_k^c|\hat{u}\times r|\psi_k^v\rangle\right|^2\delta(E_k^c-E_k^v-E),$$

where ω is the light frequency, e is the electronic charge, and ψ_k^c and ψ_k^v are the conduction band (CB) and valence band (VB) wavefunctions at k, respectively. The real part $\varepsilon_1(\omega)$ of the dielectric function $\varepsilon(\omega)$ can be derived from the imaginary part $\varepsilon_2(\omega)$ using the Kramers–Kronig dispersion equation. All other optical constants on the energy dependence of the absorption spectrum, the refractive index, the extinction coefficient, the energy-loss spectrum, and the reflectivity can be derived from $\varepsilon_1(\omega)$ and $\varepsilon_2(\omega)$ [16].

3. Results and discussions

3.1. Structural and elastic properties

$BiAlO_3$ belongs to the space group R3c. We used X-ray powder diffraction data [10] as a starting point for geometry optimization. We calculated the structural parameters for the hexagonal and cubic $BiAlO_3$, respectively. The results are summarized in Table 1. For the hexagonal $BiAlO_3$, the lattice parameters a and c are smaller than the experimental values by 1.7% and 1.1%, respectively. These deviations are within the admitted range of the errors of the first-principles method. For the cubic $BiAlO_3$, our results are in good agreement with the results that Wang et al. [11] calculated by using an accurate FP-LAPW method. It can be seen that the optimized hexagonal structure is reasonable. It is also found that ultrasoft Vanderbilt-type pseudopotentials are appropriate for studying $BiAlO_3$ material.

Table 1
The lattice parameters of $BiAlO_3$

			$a=b$ (Å)	c (Å)	V (Å^3)
$BiAlO_3$	Hexagonal	Calculated[a]	5.29	13.24	320.24
		Experimental[b]	5.38	13.39	335.16
	Cubic	Calculated[a]		3.68	
		FP-LAPW–GGA[c]		3.75	

[a]This work.
[b]Ref. [10].
[c]Ref. [11].

Table 2
The calculated bulk modulus B_0 (GPa), elastic constants (GPa) for hexagonal $BiAlO_3$

$BiAlO_3$			
B_0	140.55	C_{13}	34.85
C_{11}	301.66	C_{33}	300.86
C_{12}	118.85	C_{44}	68.54

For hexagonal crystals, the mechanical stability requires the elastic constants satisfying the well-known Born stability criteria [17]:

$$C_{11}>0,\quad C_{11}-C_{12}>0,\quad C_{44}>0,$$
$$(C_{11}+C_{12})C_{33}-2C_{13}^2>0.$$

From our calculated C_{ij} shown in Table 2, it is known that the hexagonal $BiAlO_3$ is mechanically stable. To the best of our knowledge, no experimental or theoretical data for the elastic constants of $BiAlO_3$ are available. Therefore, we consider the present results as a prediction study.

3.2. Electronic properties

The energy band structure, total density of states, and partial densities of states for hexagonal $BiAlO_3$ are shown in Figs. 1–3, respectively. The top of the VB and the bottom of the CB are composed of O 2p states and Bi 6p states, respectively. In contrast, the band gap of $PbTiO_3$ ($PbZrO_3$) is determined by O 2p states and Ti 3d (Zr 4d) states rather than those associated with Pb–O. The VB maximum locates between G and M points. On the other hand, the CB minimum locates at M point. Therefore, $BiAlO_3$ presents an indirect band gap of 3.28 eV. The band gaps predicted by DFT are smaller than experimental data, which means that our result underestimates the real band gap of $BiAlO_3$. In our calculation, the scissors operator

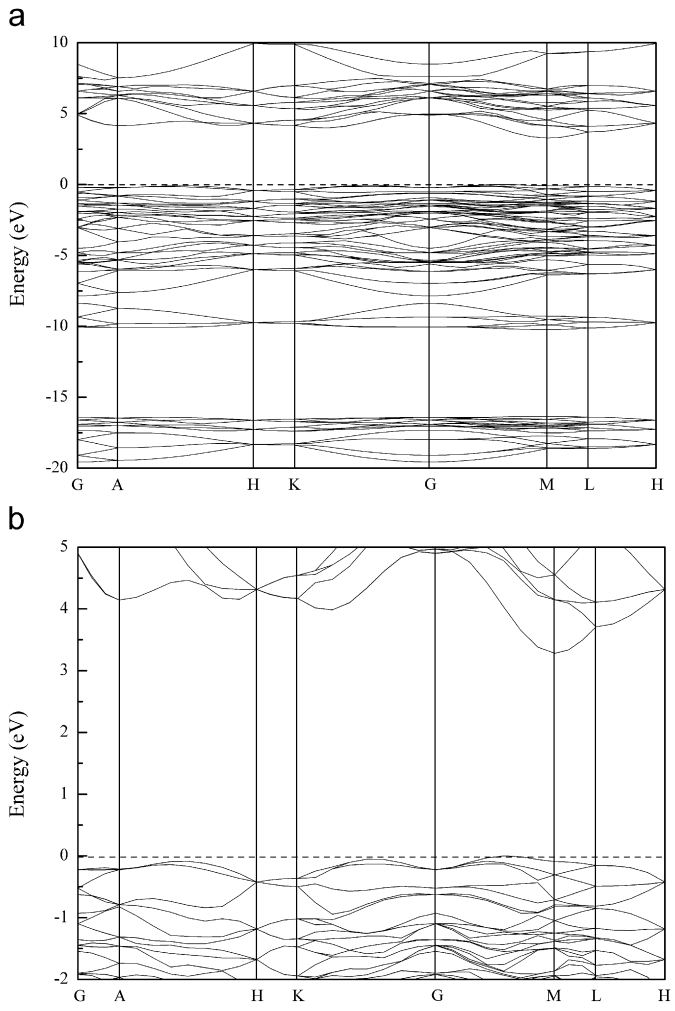

Fig. 1. (a) Band structure of hexagonal $BiAlO_3$ and (b) a magnified view of the band structure around the Fermi level.

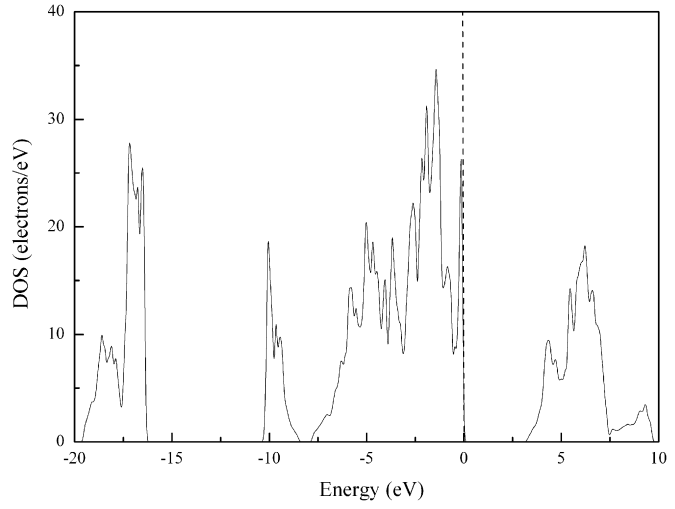

Fig. 2. Total density of states of hexagonal $BiAlO_3$.

(SO) on both the electronic structure and the optical properties is not considered. The lower VB formed by O 2s states is about −17 eV with a bandwidth of 4 eV. The Bi 6s

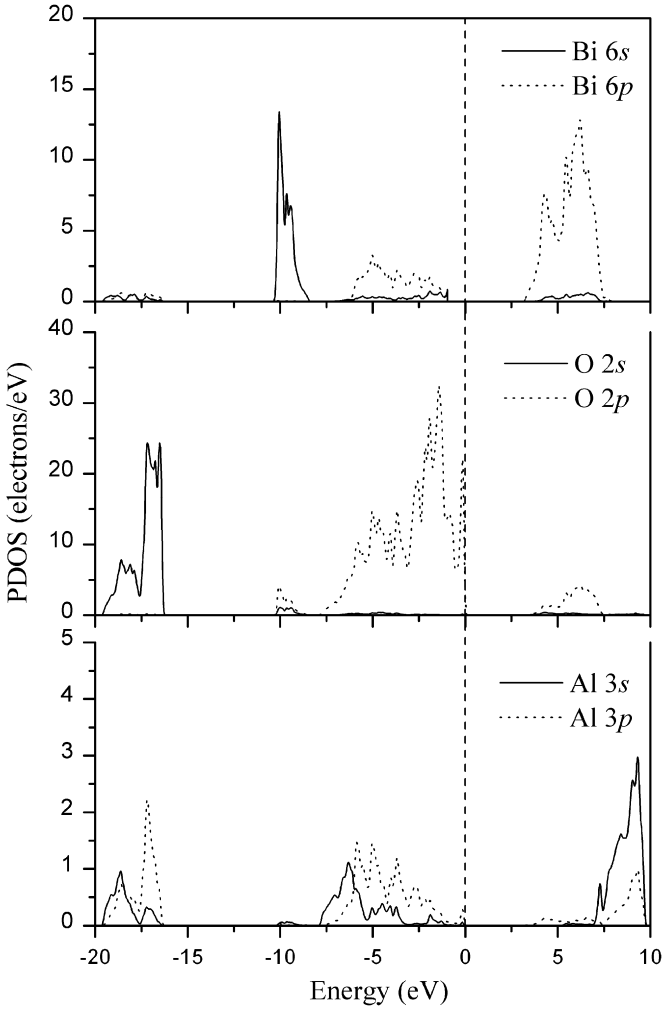

Fig. 3. Partial density of states of hexagonal $BiAlO_3$.

states are located at about −10 eV having a bandwidth of 2 eV. By analyzing partial density of states, it is found that the O 2p states have some admixture with the Bi p and Al sp states. It can be seen that $BiAlO_3$ has some covalent features. Moreover, in the region of the VB, the width of the PDOS of Bi is clearly narrower than that of Al and O. The number of peaks is also less than those for Al. This result indicates that the hybridization of Al–O is stronger than that for Bi–O. Above 6 eV and up to 10 eV, the energy bands derived from the Al 3p and 3s states that force Bi 6p states to move toward the Fermi level. Based on the foregoing results, it is found that the electronic properties of $BiAlO_3$ are affected by the Al ion through their influence on the Bi–O bonding.

By comparing the electronic properties of $BiAlO_3$ in hexagonal and cubic phases [11], it can be seen that the band gaps of these two phases are quiet different. The energy gap for hexagonal phase (3.28 eV) is larger than that for cubic phase (1.57 eV). The electronic properties of these two phases have also some similar features: (i) both hexagonal and cubic $BiAlO_3$ have a strong covalent bonding; (ii) their electronic properties are affected by the

Table 3
Mulliken charge population of hexagonal $BiAlO_3$

Species	Charge (electron)		Bond lengths (Å)	Bond populations
Bi	1.53	O–Al	1.84	0.42
Al	1.50	O–Bi	2.19	0.14
O	−1.01	O–O	2.58	−0.14
		Al–Bi	2.91	−0.19

Al ion through their influence on the Bi–O bonding; (iii) the top of VB and the bottom of CB are mainly formed by O 2p states and Bi 6p states, respectively.

We also performed the Mulliken charge populations for $BiAlO_3$ because it is a good method to understand bonding behavior. The Mulliken charge populations are given in Table 3. The charge transfer from Bi and Al to O is about 1.53 and 1.50 electrons, respectively. The bond populations indicate the overlap degree of the electron cloud of two bonding atoms [18]. Its highest and lowest values imply that the chemical bond exhibits strong covalency and ionicity, respectively. Therefore, we concluded that the bonding behavior of $BiAlO_3$ is a combination of covalent and ionic nature. Moreover, the Al–O bond possesses the stronger covalent bonding strength than the Bi–O bond. The results are consistent with our DOS calculation. The negative values of bond population for O–O and Al–Bi imply that these bonds have the tendency to be broken or have Van der Waals interaction only.

3.3. Optical properties

Fig. 4 shows the calculated dielectric function of $BiAlO_3$. The imaginary part $\varepsilon_2(\omega)$ of the dielectric function has five prominent peaks. Peak A (4.65 eV) corresponds to the transition from O 2p VB to states in CB with a small contribution from Bi 6s states, and peaks B (6.03 eV) and C (7.87 eV) correspond to the transition from O 2p VB to Al 3s CB. Peaks D (14.46 eV) and E (18.12 eV) are ascribed to the transition of inner electron excitation from O 2s and Bi 6s levels to CB. The calculated static dielectric constant $\varepsilon_1(0)$ is 5.81, which is larger than those of $BaTiO_3$ (5.12), $SrTiO_3$ (4.98), and $PbZrO_3$ (5.34). It is reasonable to expect that $BiAlO_3$ is a promising dielectric material.

Fig. 5(a)–(e) shows the calculated results on the absorption spectrum, refractive index, extinction coefficient, reflectivity, and energy-loss spectrum, respectively. In our calculation, we used a 0.3 eV Gaussian smearing. The absorption spectrum starts at 3.57 eV and decreases rapidly in the low-energy region. In the range from 0 to 3.57 eV, the reflectivity is lower than 20%, which indicates that $BiAlO_3$ material is transmitting for frequencies less than 3.57 eV. The energy-loss spectrum describes the energy loss of a fast electron traversing in the material [19]. Its main peak is generally defined as the bulk plasma frequency ω_p, which occurs where $\varepsilon_2 < 1$ and ε_1 reaches the zero point [20,21]. Moreover, the main peak at about 25.38 eV

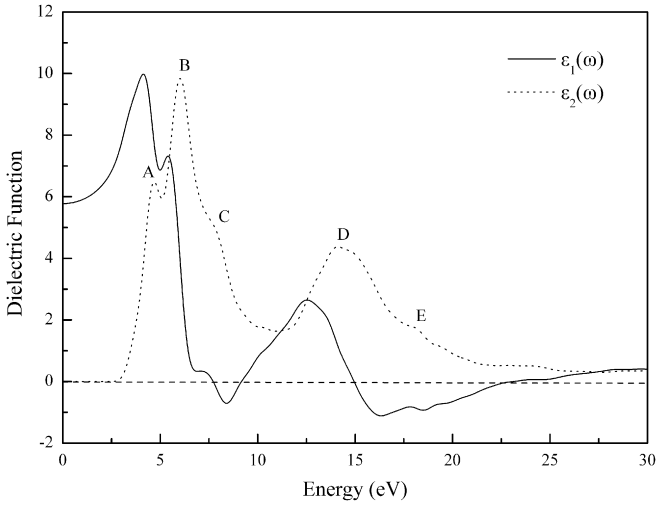

Fig. 4. The calculated imaginary part $\varepsilon_2(\omega)$ and real part $\varepsilon_1(\omega)$ of the dielectric function $\varepsilon(\omega)$ for hexagonal $BiAlO_3$.

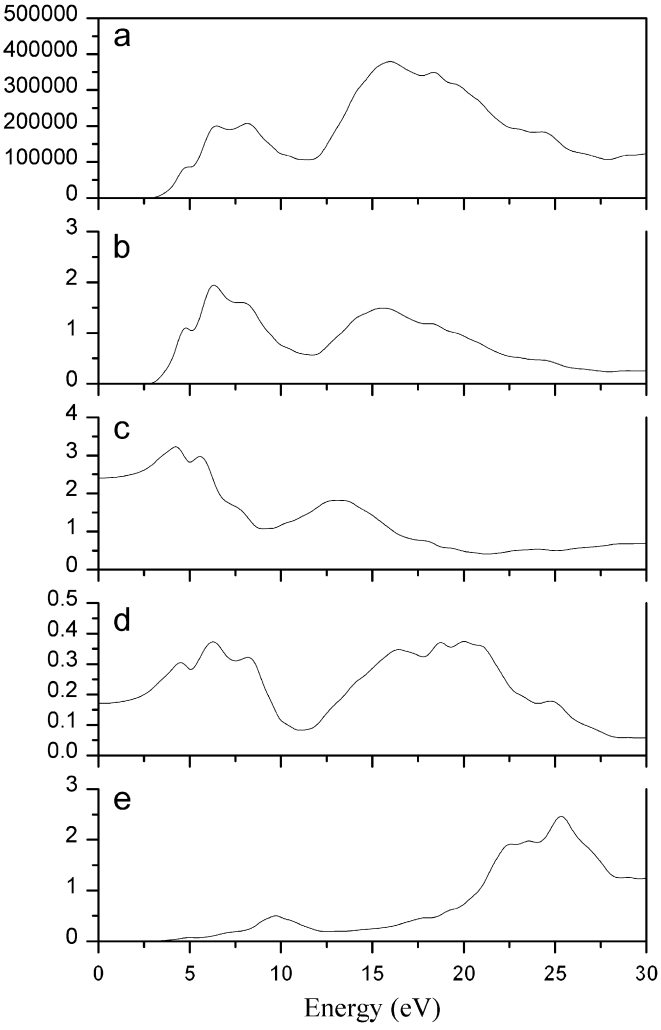

Fig. 5. The calculated optical constants for hexagonal $BiAlO_3$: (a) Absorption spectrum, (b) refractive index, (c) extinction coefficient, (d) reflectivity, and (e) energy-loss spectrum.

corresponds to a rapid reduction of the reflectance. This process is associated with the transitions from the filled O 2s bands to empty CB. The calculated static refractive index is equal to 2.39.

4. Conclusions

In summary, the structural parameters, elastic constants, electronic structures, and optical properties of hexagonal $BiAlO_3$ were studied by the DFT within the GGA. Our structural parameters are in good agreement with previous calculation and experimental data. The calculated elastic constants indicated that $BiAlO_3$ is mechanically stable. The electronic structures of $BiAlO_3$ reveal that the top of the VB and the bottom of the CB are decided by O 2p and Bi 6p states, respectively. $BiAlO_3$ presents an indirect band gap of 3.28 eV. Furthermore, the Al–O bond possesses the stronger covalent bonding strength than the Bi–O bond. Finally, the dielectric function, absorption spectrum, refractive index, extinction coefficient, reflectivity, and energy-loss spectrum are obtained. It is found that $BiAlO_3$ may be promising dielectric materials. The relations of the optical properties to the interband transitions are also discussed.

Acknowledgments

This work was supported by the National Natural Science Foundation of China (10572155, 10172030, 50232030) and the Science Foundation of Guangdong Province (2005A10602002).

References

[1] M. Fiebig, J. Phys. D: Appl. Phys. 38 (2005) R123.
[2] N.A. Hill, J. Phys. Chem. B 104 (2000) 6694.
[3] R.E. Eitel, S.J. Zhang, T.R. Shrout, C.A. Randall, I. Levin, J. Appl. Phys. 96 (2004) 2828.
[4] S.J. Zhang, C.A. Randall, T.R. Shrout, Appl. Phys. Lett. 83 (2003) 3150.
[5] S.V. Halilov, M. Fornari, D.J. Singh, Phys. Rev. B 69 (2004) 174107.
[6] R.E. Eitel, C.A. Randall, T.R. Shrout, P.W. Rehrig, W. Hackenberger, S.-E. Park, Jpn. J. Appl. Phys. 40 (2001) 5999.
[7] J. Iniguez, D. Vanderbilt, L. Bellaiche, Phys. Rev. B 67 (2003) 224107.
[8] J. Wang, J.B. Neaton, H. Zheng, V. Nagarajan, S.B. Ogale, B. Liu, D. Viehland, V. Vaithyanathan, D.G. Schlom, U.V. Waghmare, N.A. Spaldin, K.M. Rabe, M. Wuttig, R. Ramesh, Science 299 (2003) 1719.
[9] P. Baetting, C.F. Schelle, R. LeSar, U.V. Waghmare, N.A. Spaldin, Chem. Mater. 17 (2005) 1376.
[10] A.A. Belik, T. Wuernisha, T. Kamiyama, K. Mori, M. Maie, T. Nagai, Y. Matsui, E. Takayama-Muromachi, Chem. Mater. 18 (2006) 133.
[11] H. Wang, B. Wang, R. Wang, Q.K. Li, Phys. B 390 (2007) 96.
[12] J.P. Perdew, K. Burke, M. Ernzerhof, Phys. Rev. Lett. 77 (1996) 3865.
[13] D. Vanderbilt, Phys. Rev. B 41 (1990) 7892.
[14] M.D. Segall, C.J. Pickard, R. Shah, M.C. Payne, Phys. Rev. B 54 (1996) 16317.
[15] H.J. Monkhorst, J.D. Pack, Phys. Rev. B 13 (1976) 5188.
[16] S. Saha, T.P. Sinha, A. Mookerjee, Phys. Rev. 62 (2000) 8828.
[17] Q.K. Hu, Q.H. Wu, Y.M. Ma, L.J. Zhang, Z.Y. Liu, J.L. He, H. Sun, H.T. Wang, Y.J. Tian, Phys. Rev. B 73 (2006) 214116.
[18] J. Sun, X.F. Zhou, Y.X. Fan, J. Chen, H.T. Wang, Phys. Rev. B 73 (2006) 045108.
[19] Z.W. Chen, M.Y. Lv, L.X. Li, Q. Wang, X.Y. Zhang, R.P. Liu, Thin Solid Films 515 (2006) 2433.
[20] J.S. de Almeida, R. Ahuja, Phys. Rev. B 73 (2006) 165102.
[21] M. Xu, S.Y. Wang, G. Yin, J. Li, Y.X. Zheng, L.Y. Chen, Appl. Phys. Lett. 89 (2006) 151908.